Comprehensive Laser-induced Incandescence (LII) modeling for soot particle sizing

Joel Lisanti[1, *], Emre Cenker[1], William L. Roberts[1]

[1] Clean Combustion Research Center, King Abdullah University of Science and Technology, Thuwal, Saudi Arabia

Abstract
To evaluate the current state of the art in LII particle sizing, a comprehensive model for predicting the temporal incandescent response of combustion-generated soot to absorption of a pulsed laser is presented. The model incorporates particle heating through laser absorption, thermal annealing, and oxidation at the surface as well as cooling through sublimation and photodesorption, radiation, conduction and thermionic emission. Thermodynamic properties and the thermal accommodation coefficient utilized in the model are temperature dependent. In addition, where appropriate properties are also phase dependent, thereby accounting for annealing effects during laser heating and particle cooling.

Introduction

In combustion, soot is of major concern because of the stringent regulations of particulate matter emission. Meeting these regulations requires the understanding of formation, growth, aggregation, and oxidation of soot. A quantitative understanding of these processes enables the development of methodologies to limit pollutant emissions and to develop soot prediction models to be used in CFD (computational fluid dynamics) codes [1,2]. The primary soot particle diameter d_p is one key indicator for interpreting the effects of soot formation and burnout.

Time-resolved laser-induced incandescence (TiRe-LII) emerged as a powerful *in situ* technique for measuring particle sizes. Soot particles are heated via absorption of light from a laser pulse to temperatures well above flame temperature and the subsequent blackbody radiation is recorded with fast photomultipliers (PMT) in combination with a transient recorder, such as a digital storage oscilloscope during the heat-up and cooling phase. Particle-size information can be obtained from a best-fit comparison of the temporal signal decay and simulations based on the particle's energy and mass balance equations [3,4].

Considerable effort has been devoted to developing models capable of predicting LII signals in response to pulsed laser heating over a range of fluences. Many researchers have implemented the underlying equations into their inhouse software. Michelsen et al. [3] compared the results from ten different models from various research groups in order to assess the state of understanding of the mechanisms involved and the uncertainties in the analysis of LII data. Large variability was observed in signal decay rates among these models. Some of these codes have the focus in defining of all the possible heat and mass exchange mechanisms [5,6], whereas some codes simplify such physics but focus on other controlling parameters such as pressure [4] or particle-size dispersion [7]. However a comprehensive approach that implements all effective factors was lacking.

In this work we developed a new simulation software that incorporates modeling of various physical and chemical interactions for predicting the temporal response of the particle to pulsed laser heating. The model includes particle heating through absorption of laser light, thermal annealing, and oxidation at the surface as well as cooling through sublimation and photodesorption of C_1-C_5 clusters, radiation, conduction and thermionic emission. At the current stage relevant models shown in ref. [5] are used to describe the particle's energy and mass balance equations.

Particle density, specific heat, and the thermal accommodation coefficient utilized in the model are temperature dependent. In addition, thermodynamic and optical properties are phase dependent meaning that they are changing due to the annealing effects during laser heating and particle cooling. In order to account for changes in the temperature of the bath gas surrounding the particles, local gas heating [8] is included in the model and shown to produce a meaningful effect at low fluences where cooling through conduction is dominant. Particle mass loss is accounted for through photodesorption, sublimation and oxidation terms. Polydispersed primary particles [9] and aggregate effects [10] are included and a new method for including aggregate effects in the sublimation, photodesorption, and oxidation terms is developed. The C++ code used for this work is highly modular, allowing for easy expansion and adaptation, and is packaged with an intuitive GUI interface.

Particularly in this paper we evaluate the performance of the annealing subroutine [5] embedded in the new software, and investigate the overall effects of this annealing process on particle sizing with LII modeling. An approach of using multiple laser pulses [11–13] is implemented in the simulations. The response of LII signal and particle temperature under different two-pulse heating scenarios are analyzed.

Modeling

Soot particles undergo a thermal annealing process due to the rapid laser pulse heating and consecutive cooling in LII which leads a permanent transformation of the soot morphology and a change of its optical properties. Although it is proven that annealing takes place at all laser fluences and could have a significant impact on LII signals [13], still little is known about this mechanism. Overall effects of this annealing process on particle sizing with LII modeling are investigated by measuring the time-resolved (TiRe) LII signal decay from in-flame soot.

Laser absorption is modeled as the product of the normalized laser intensity profile weighted by the laser fluence and the absorption cross-section as detailed in [5]. In this model the absorption cross-section is computed as diameter, wavelength, and annealed mass fraction dependent. Heat loss through radiation is modeled by the Planck equation with an emissivity correction accounting for annealing as described in [5].

Thermal annealing is modeled following the work of H.A. Michelsen and is described in detailed in [5]. In this work annealing occurs at temperatures high enough to allow for migration of interstitial carbon atoms in a process known as Frenkel defect annihilation. Also, at even higher temperatures clustering of lattice vacancies is modeled as Schottky defect annihilation. Thus, the annealing rate is computed as the rate of defect formation minus the rates of defect annihilation given in Eq. 1 and Eq. 2. In this equation N_d is the number of defects, N_p is the number of atoms in the particle, X_d is the initial defect density of the particle, k_{diss} is the rate constant for pyrolysis of the annealed particle, k_{imig} is the rate constant for interstitial migration, k_{vmig} is the rate constant for vacancy migration, and X_{ann} is the mass fraction of the particle that has been annealed.

$$\frac{dN_d}{dt} = X_{ann}\frac{N_p}{2}k_{diss} - k_{imig}N_d - k_{vmig}N_d \qquad \text{Eq. 1}$$

$$X_{ann} = 1 - \frac{N_d}{X_d N_p} \qquad \text{Eq. 2}$$

Sublimation and photodesorption of carbon clusters C_1-C_5 is included in the model as used by H.A. Michelsen in [3]. In addition heat loss through conduction and heat production/mass loss through oxidation are included as detailed in [5]. Thermophysical particle properties and the thermal accommodation coefficient, as given in [11], are temperature and annealed mass fraction dependent. For the purposes of this study aggregate modeling and polydisperion were switched off as it is useful to isolate the physics of a single isolated particle. The bath gas temperature was taken to be 1900 K and the pressure was set to 1 bar. Primary particle diameters were set at 35 nm for all simulations.

Results

In a two-pulse LII system, where soot is preheated, hence annealed, with the first pulse, the LII signal decay after the consecutive second pulse is a sensitive measure to particle annealing. In effort to design two-pulse LII experiments and gain insight into the behavior of the LII model, preliminary simulations were carried out. These simulations may be used to identify regimes of two-pulse LII in which the effects of annealing may be isolated and thus are relevant for experimental investigation into annealing effects. In each case the simulations are comprised of two laser pulses, the first with a Gaussian temporal profile and 7 ns full-width at half-maximum and the second with a 2 ns top-hat profile. Each laser is used at a wavelength of 1064 nm. These profiles are chosen to be representative of the equipment available in the KAUST Clean Combustion Research laboratory and will be used in future two-pulse LII experiments.

In the first case the fluence of each laser was kept constant at 0.05 J/cm^2. Such a low fluence is deliberately chosen to avoid sublimation. In order to investigate the annealing time scales, the separation between each pulse was varied from 50 ns to 550 ns and the resulting LII signal is shown in Fig. 1. It is observed in Fig. 1 that the relative decrease in peak LII signal with increasing separation appears to be also decreasing. Thus, it is suggesting that the increase in annealed mass fraction of the particle is increasing the particles' sensitivity to laser irradiation, as seen in previous studies [12]. This is not the case, however, as the model decreases the sensitivity of the particle to laser irradiation with increasing annealed mass fraction.
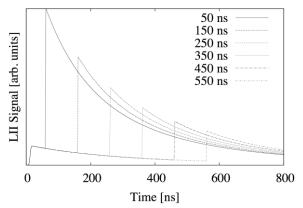

Fig. 1 Simulated LII signal for constant fluence, two-pulse LII with separation between laser pulses varying from 50 ns to 550 ns

The temporal profile of the particles' annealed mass fraction is plotted for each case in Fig. 2. It is shown that, as the separation between the laser pulses is increased; the annealed mass fraction of the second particle at the start of the second pulse is also increased. As such, the absorption characteristics of the particle are altered and thus the resulting LII signal profile is modified directly due to annealing and the initial temperature of the particle.
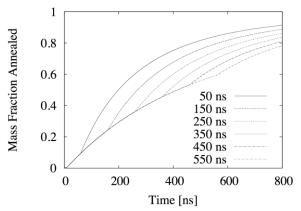
2

Fig. 2 Particle annealed mass fraction for constant fluence, two-pulse LII with separation between laser pulses varying from 50 ns to 550 ns

The second simulated case is such that the separation between the laser pulses is held constant at 50 ns, and the fluence of the second pulse is held constant at 0.05 J/cm^2. The fluence of the first pulse is then varied from 0.025 J/cm^2 to 0.4 J/cm^2. The resulting simulated LII signal is shown in Fig. 3 and temporal evolution of annealed mass fraction in Fig. 4.
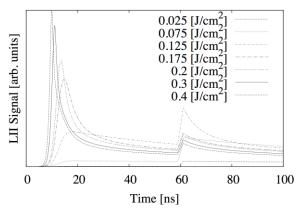

Fig. 3 Simulated LII signal for constant separation, two-pulse LII with fluences of the first pulse varying from 0.025 J/cm^2 to 0.4 J/cm^2

It is observed that, in the case in which the fluence of the first pulse is below the sublimation threshold, the peak signal resulting from the second pulse is larger than that from the first pulse. As the fluence is raised above 0.125 J/cm^2 mass losses from sublimation and photodesorption decrease the diameter of the particle to such an extent that the second peak in LII signal is significantly lower from the first. In these cases it is difficult to separate annealing effects from sublimation and photodesorption.

It is also shown in Fig. 4 that the annealed mass fraction of the particle is strongly dependent on the fluence of the first pulse. Below the sublimation threshold the particle does not fully anneal in the duration of the simulation and a change in slope is present at the time of the second pulse. For high fluence cases, above the sublimation threshold, the particle is simulated to anneal during the first pulse and thus there is no

significant change in annealed mass fraction due to the second pulse. In this case, it may then be possible to separate sublimation and photodesorption effects from annealing for model validation. In this case, if the annealed particle optical properties are known, differences in the second LII signal will primary result from mass and heat loss through sublimation.
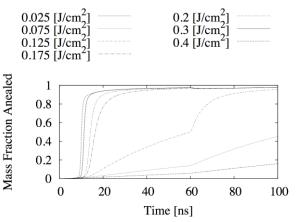

Fig. 4 Particle annealed mass fraction for constant separation, two-pulse LII with fluences of the first pulse varying from 0.025 J/cm^2 to 0.4 J/cm^2

In order to further isolate the effects of annealing a third set of simulations was carried out by simulating the response of the particle to two-pulse LII with the second pulse occurring at the time at which the particle had cooled to 2200 K. In this case the fluence of the first pulse was varied from 0.025 J/cm^2 to 0.075 J/cm^2, well below the sublimation threshold, and the second pulse fluence was held constant at 0.05 J/cm^2. The temporal temperature response is shown in Fig. 5 providing an indication of the timing of the second pulse. It is shown that the onset time of the second pulse, based on the particle temperature reaching 2200 K, increase greatly with the fluence of the first pulse. For the 0.025 J/cm^2 case the second pulse occurs at ~85 ns, and for the 0.05 and 0.075 J/cm^2 at ~1100 ns and ~1640 ns respectively.
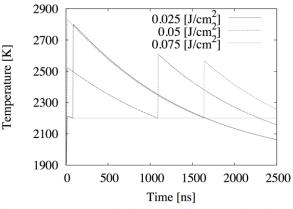

Fig. 5 Temperature of primary particle as a function of time for two-pulse LII with constant second pulse fluence and first pulse fluence varying from 0.025 J/cm^2 to 0.075 J/cm^2

It is then shown in Fig. 6 that the time of the second pulse corresponds to vastly different annealed mass fractions in each case. Thus allowing the effect of annealing, without sublimation or photodesorption, to be directly investigated and quantified. It is also noted that the time required for the particle to cool to 2200 K is none linearly dependent on the fluence. At fluences above the sublimation threshold a decrease in diameter due to mass loss will result in a reversal in the trend with time for the particle to cool to 2200 K decreasing with increasing fluence.
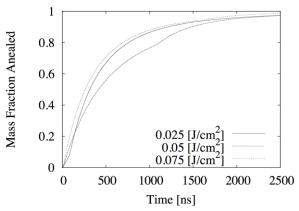

Fig. 6 Annealed mass fraction as a function of time for two-pulse LII with constant second pulse fluence and first pulse fluence varying from 0.025 J/cm^2 to 0.075 J/cm^2

The resulting simulated LII signal is then shown in Fig. 7. The peak signal resulting from the first pulse follows the expected trend with the peak increasing in magnitude with fluence. However, the second peak behaves in the opposite manner with the magnitude of the peak decreasing with increasing fluence of the first pulse. In each case the temperature of the particle at the start of the second pulse is 2200 K, the fluence of the second pulse is 0.05 J/cm^2, and the amount of mass loss due to the first pulse is negligible. The only significant difference between the second pulses is the annealed mass fraction of the particle. As described by Michelsen in [5], the annealing model utilized for this simulation results in a decreased sensitivity to laser irradiation with increased annealed mass fraction. This is observed in Fig. 7 as the magnitude of the peak LII signal is shown to decrease significantly with increasing annealed mass fraction. This directly contradicts the suggestion that annealing increases the sensitivity of the soot particles as observed experimentally in [13].
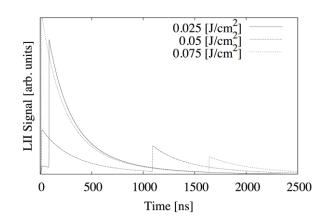

.

Fig. 7 Simulated LII signal for two-pulse LII with constant second pulse fluence and first pulse fluence varying from 0.025 J/cm^2 to 0.075 J/cm^2

Conclusions

Annealing effects may strongly influence the temporal response of a soot particle to laser irradiation. In order to quantify these effects in the context of LII particle sizing, it is necessary to obtain experimental results isolating the annealing physics. A two- pulse LII experiment utilizing two lasers has been proposed and simulation results have shown that such information should allow for the quantification of annealing effects in LII measurements.

The only current known annealing model for LII particle sizing appears to contradict the limit experimental information on soot annealing present in the literature. Future experimental studies will directly compare two-pulse simulations with two-pulse experiments to evaluate the ability of the current annealing model to capture reality.

Acknowledgements

References

[1]   C. Schulz, B.F. Kock, M. Hofmann, H.A. Michelsen, S. Will, B. Bougie, R. Suntz, G.J. Smallwood, Appl. Phys. B 83 (2006) 333–354.

[2]   E. Cenker, G. Bruneaux, L.M. Pickett, C. Schulz, SAE Int. J. Engines 6 (2013) 352–365.

[3]   H.A. Michelsen, F. Liu, B.F. Kock, H. Bladh, A. Boiarciuc, M. Charwath, T. Dreier, R. Hadef, M. Hofmann, J. Reimann, S. Will, P.-E. Bengtsson, H. Bockhorn, F. Foucher, K.-P. Geigle, C. Mounaïm-Rousselle, C. Schulz, R. Stirn, B. Tribalet, R. Suntz, Appl. Phys. B 87 (2007) 503–521.

[4]   M. Hofmann, B.F. Kock, T. Dreier, H. Jander, C. Schulz, Appl. Phys. B 90 (2007) 629–639.

[5]   H.A. Michelsen, J. Chem. Phys. 118 (2003) 7012–7045.

[6]   A. Nanthaamornphong, J.C. Carver, K. Morris, H.A. Michelsen, D.W.I. Rouson, Comput. Sci. Eng. 16 (2014) 36–46.

[7]   F. Liu, M. Yang, F.A. Hill, D.R. Snelling, G.J. Smallwood, Appl. Phys. B 83 (2006) 383–395.

[8]   E. Nordström, N.-E. Olofsson, J. Simonsson, J. Johnsson, H. Bladh, P.-E. Bengtsson, Proc. Combust. Inst. 35 (2015) 3707–3713.

[9]   E. Cenker, G. Bruneaux, T. Dreier, C. Schulz, Appl. Phys. B, in press (2014).

[10]   F. Liu, Smallwood, D.R. Snelling, J. Quant. Spectrosc. Radiat. Transf. 93 (2005) 301–312.

[11]   S. Iuliis, F. Cignoli, S. Maffi, G. Zizak, Appl. Phys. B 104 (2011) 321–330.

[12]   R.L. Vander Wal, K.A. Jensen, Appl. Opt. 37 (1998) 1607–1616.

[13]   R.L. Vander Wal, T.M. Ticich, A.B. Stephens, Appl. Phys. B 67 (1998) 115–123.